Accepted Manuscript

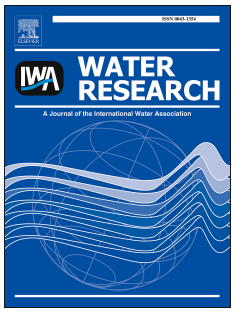

Effect of dissolved oxygen concentration on iron efficiency: Removal of three chloroacetic acids

Shun Tang, Xiao-mao Wang, Yu-qin Mao, Yu Zhao, Hong-wei Yang, Yuefeng F. Xie

PII: S0043-1354(15)00055-X

DOI: 10.1016/j.watres.2015.01.027

Reference: WR 11119

To appear in: *Water Research*

Received Date: 4 November 2014

Revised Date: 11 January 2015

Accepted Date: 20 January 2015

Please cite this article as: Tang, S., Wang, X.-m., Mao, Y.-q., Zhao, Y., Yang, H.-w., Xie, Y.F., Effect of dissolved oxygen concentration on iron efficiency: Removal of three chloroacetic acids, *Water Research* (2015), doi: 10.1016/j.watres.2015.01.027.

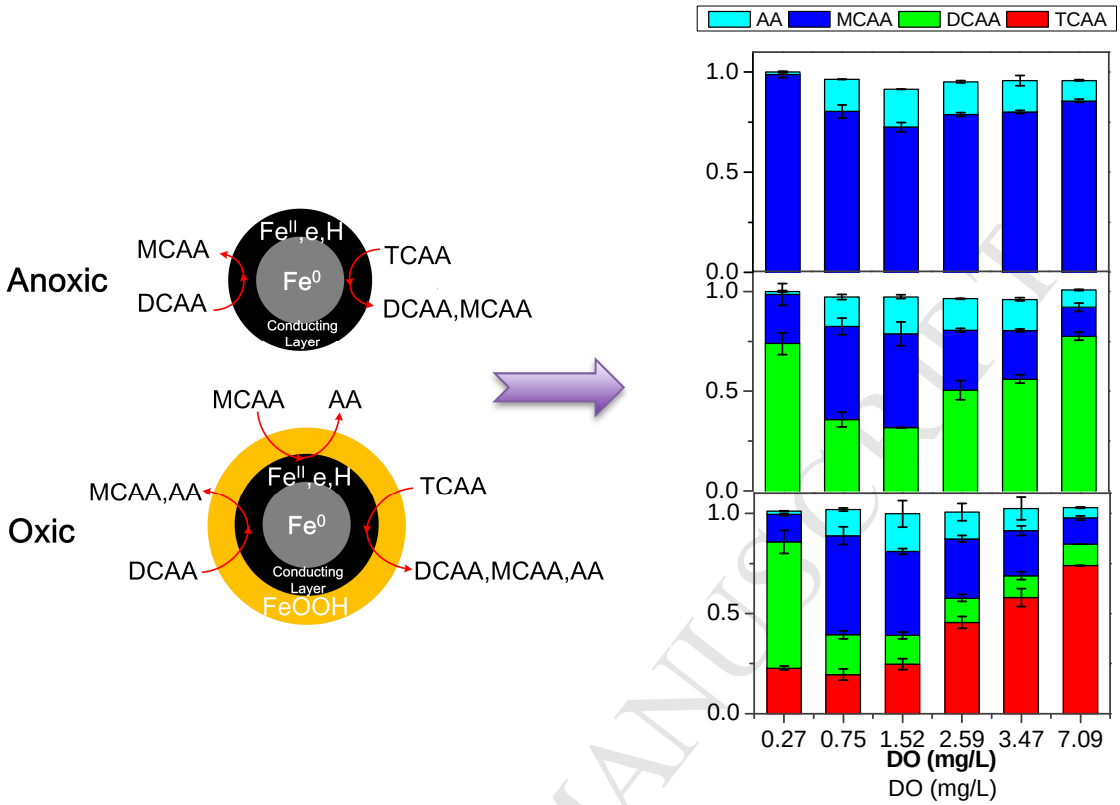

Effect of dissolved oxygen concentration on iron efficiency: Removal of three chloroacetic acids

Shun Tang[1], Xiao-mao Wang[1], Yu-qin Mao[1], Yu Zhao[1], Hong-wei Yang[1,*], Yuefeng F. Xie[1,2]

[1]State Key Joint Laboratory of Environmental Simulation and Pollution Control, School of Environment, Tsinghua University, Beijing 100084, P.R. China

[2]Environmental Programs, The Pennsylvania State University, 777 West Harrisburg Pike, Middletown, PA17057, USA

Re-submitted to

Water Research

October, 2014

*Corresponding author.

Address: School of Environment, Tsinghua University, Beijing 100084, People's Republic of China.

Tel.: +86-10-6277 2987

Email: yanghw@tsinghua.edu.cn (H.W. Yang)

Abstract

The monochloroacetic, dichloroacetic and trichloroacetic acid (MCAA, DCAA and TCAA) removed by metallic iron under controlled dissolved oxygen conditions (0, 0.75, 1.52, 2.59, 3.47 or 7.09 mg/L DO) was investigated in well-mixed batch systems. The removal of CAAs increased first and then decreased with increasing DO concentration. Compared with anoxic condition, the reduction of MCAA and DCAA was substantially enhanced in the presence of O_2, while TCAA reduction was significantly inhibited above 2.59 mg/L. The 1.52 mg/L DO was optimum for the formation of final product, acetic acid. Chlorine mass balances were 69-102%, and carbon mass balances were 92-105%. With sufficient mass transfer from bulk to the particle surface, the degradation of CAAs was limited by their reduction or migration rate within iron particles, which were dependent on the change of reducing agents and corrosion coatings. Under anoxic conditions, the reduction of CAAs was mainly inhibited by the available reducing agents in the conductive layer. Under low oxic conditions, the increasing reducing agents and thin lepidocrocite layer were favorable for CAA dechlorination. Under high oxic conditions, the redundant oxygen competing for reducing agents and significant lepidocrocite growth became the major restricting factors. Various CAA removal mechanisms could be potentially applied to explaining the effect of DO concentration on iron efficiency for contaminant reduction in water and wastewater treatment.

Keywords: Dissolved oxygen (DO); Iron; Corrosion products; Removal mechanism;

Chloroacetic acids

1. Introduction

In recent years, zero valent iron (Fe^0) and Fe^0-doped particles have been shown very efficient for the aqueous removal of various inorganic and organic contaminants (Cundy et al., 2008; Fu et al., 2014; Gunawardana et al., 2011; Henderson et al., 2007; Li et al., 2006; Noubactep, 2008; Scott et al., 2011). The potential effect of the coexisting oxidants on iron corrosion, such as oxygen (O_2) or chlorine, has attracted considerable attention (Jung et al., 2011; Rahman and Gagnon, 2014; Sarin et al., 2004a, 2004b; Stratmann and Müller, 1994; Wang et al., 2012; Zhang and Huang, 2006). However, limited investigation have been completed examining the influence of O_2 on the removal of contaminants by iron (Ghauch et al., 2010, 2011; Huang and Zhang, 2005; Wang et al., 2010). The rate constant for carbon tetrachloride reacting with iron under an oxic condition was significantly lower than that under an anoxic condition (Helland et al., 1995). The presence of O_2 in the iron-water system decreased the removal efficiency of nitrate (Westerhoff and James, 2003) and bromate (Xie and Shang, 2007), and slowed the reduction of bromoacetic acid (Zhang et al., 2004), trichloropropanone (Lee et al., 2007) and diclofenac (Ghauch et al., 2011). The rapid removal of carbon tetrachloride and trichloroethylene using iron and palladized-iron cathodes was not interfered even when purging the raw water with air (Li and Farrell, 2000). The nitrate reduction could maintain stable under various oxic conditions if amending iron with the aqueous ferrous ion (Huang and Zhang, 2005).

The existing O_2 failed to inhibit with the quick degradation of tribromoacetic acid, trichloronitromethane and trichloracetonitrile, which were mass transfer limited species (Lee et al., 2007; Zhang et al., 2004). Some attractive results have been reported on the enhancing effect of O_2 on iron efficiency for the removal of dye (Wang et al., 2010) and diclofenac (Ghauch et al., 2010) in a batch system, and the reduction of nitrate (Westerhoff and James, 2003) and chromium (Yoon et al., 2011) in a packed column.

A potential mechanism for different O_2 roles was involved the formation of various iron corrosion products, which served as a physical barrier, a semiconductor or a coordinating surface in the core-shell structure of iron corrosion (Scherer et al., 1998; Sarin et al., 2004a; Yan et al., 2010). Uludag-Demirer and Bowers (2003) reported O_2 acted as an irreversible inhibitor of the trichloroethylene reduction based on the assumption of magnetite and maghemite formed on the iron surface. Huang and Zhang (2005) reported maghemite or lepidocrocite produced under oxic conditions would decrease the removal efficiency of iron, while magnetite even in a substantial thickness might not impede the nitrate reduction. In these researches, Fe^0 was widely regarded as an effective reductant (direct reduction), which was responsible for the decrease of contaminants (Gillham and O'Hannesin, 1994; Li et al., 2006; Matheson and Tratnyek, 1994). Due to ubiquitous oxide films decreasing the accessibility of iron surface, the observed removal of contaminants was predominantly mediated by aqueous and/or solid corrosion products through adsorption, co-precipitation and subsequent indirect reduction by other reducing

agents except for Fe^0 (Noubactep, 2008, 2010, 2011, 2014; Noubactep et al., 2010). The reducibility of aqueous and solid iron corrosion was usually ignored, although the aqueous, absorbed or structural divalent iron (Fe^{II}) was thermodynamically capable of reducing some pollutants (Chun et al., 2005, 2007; Pecher et al., 2002; Schlautman and Han, 2001; White and Peterson, 1996). The enhancement on removal efficiency of iron was reported with coexisting iron minerals, such as magnetite (Coelho et al., 2008; Huang and Zhang, 2006; Mak et al., 2011), green rust (Cho et al., 2010), pyrite (Kim et al., 2013) and ferric hydroxide (Song et al., 2013). The availability of aqueous or solid Fe^{II} mentioned above was almost conducted under anoxic condition to restrain the rapid oxidation of Fe^{II} by O_2. Hence, the evolution of reducing ability or agents for contaminants in iron/water system under various oxic conditions was necessary to investigate in order to promote its application in the treatment of surface water and wastewater.

As important byproducts of the chlorination of water and wastewater, the chloroacetic acids (CAAs) including monochloroacetic acid (MCAA), dichloroacetic acid (DCAA) and trichloroacetic acid (TCAA) were selected as the model compounds. The batch experiments with a controlled DO concentration ranged from 0 to 7.09 mg/L were analyzed over a 2-h reaction period, during which the liquid and solid were periodically sampled to determine the evolution of CAA degradation processes and iron corrosion products. The removal mechanism of CAAs affected by various DO concentrations was also explored in the iron/water system.

2. Materials and methods

2.1. Chemicals

The analytically pure MCAA, DCAA and TCAA were bought from the Tianjin Fuchen Chemical Regents and Sinopharm Chemical Reagent (China), respectively. The standard solution for CAAs (2000 mg/L each), formic acid, ammonium formate and sodium carbonate (analytical reagent) were purchased from Sigma-Aldrich (USA). The chromatographically pure methanol and acetonitrile were obtained from Fisher Chemicals (USA). The analytically pure sodium chloride, hydrochloric acid, sodium hydroxide, ferrous chloride and magnetite were bought from Beijing Chemical Works (China). Akaganeite substituted for lepidocrocite was synthesized for convenience (Chitrakar et al., 2006).

2.2. Iron pretreatment

The raw iron particles were collected from a local manufacturing factory, which had some grease on the surface. The particles were first passed through two sieves (0.2 and 1.0 mm), then soaked in a detergent solution for 24 h for oil removal, then rinsed in sequence with tap water, deionized water and ultrapure water for residual detergent removal, and finally stored in ultrapure water. The final iron particles contained black coatings and the specific surface area measured via BET was 1.50 m^2/g. Fresh iron without oxide films was prepared with 1 M hydrochloric acid lasting for 10 min, then rinsed with deoxygenated water until no chlorine ion detected in water.

2.3. Dissolved oxygen control

Refreshing the headspace at a 10-min interval was an effective way to maintain a

stable DO concentration in the reactor. This operation consisted of the following steps. (1) A reactor was taken down from the rotator. (2) Two needles were inserted through the silicone stopper of the reactor and one of them was connected with high-purity nitrogen gas (N_2) lasting for 20 s. (3) A specific amount of O_2 was injected into the headspace. (4) Two needles were palled out after waiting for 3-5 s, ensuring that the gas pressure in the reactor was the same as ambient pressure. The volume of adopted O_2 included 0, 0.5, 2, 5 and 8 mL and a stream of O_2 was used to provide the highest DO concentration.

2.4. Experimental System

The initial solution containing approximately 25 μM CAA was prepared using ultrapure water. After adjusting pH to 7.0 with NaOH and HCl, CAA solution was purged with N_2 for 1 h. Deoxygenated CAA solutions (55 mL) and iron particles (0.55 g) were transferred into a 65-mL brown bottle. The bottle was sealed a screw thread cap with PTFE-faced silicone septa, then supplied with O_2, and finally loaded onto a rotator at 40 rpm. The samples were collected at 0, 5, 10, 20, 30, 45, 60, 75, 90 and 120 min. Approximately 2 mL samples were preferentially withdrawn from the sealed reactor for prompt DO measurement. A certain amount of solutions, after passing through a 0.2 μm pore size syringe-mounted filter, were collected for the chemical concentration analyses. The suspended precipitates in water and corrosion coatings on iron surface were collected to analyze their physical properties. All batch experiments were performed at room temperature (25 ± 1 °C). In this paper, data represented the mean and standard deviation of duplicates.

2.5. Analytical methods

MCAA, DCAA and TCAA were determined by LCMS without pretreatment. A high-performance liquid chromatography (Agilent 1290, USA) was equipped with an Agilent Eclipse Plus C8 RRHD (1.8 μm × 2.1 mm × 50 mm). The two mobile phases were pure methanol and ultrapure water containing 0.1% formic acid and 0.125 mM ammonium formate. A triple-quadrupole mass spectrometer (Agilent 6460, USA) was equipped with an electrospray ionization source operated in the negative ion mode. The optimized mass spectrometry parameters were summarized as follows: gas temperature of 300 °C, gas flow of 7 L/min, nebulizer pressure of 35 psi, sheath gas heater temperature of 325 °C, sheath gas flow of 11 L/min; capillary voltage of 0 V. The precursor and product ion for MCAA were *m/z* 93 and *m/z* 35.1, and those for DCAA were *m/z* 127 and *m/z* 83 and those for TCAA were *m/z* 116.9 and *m/z* 35.

AA and chloride ion were analyzed using an IC (Metrohm 761, Switzerland) coupled with a conductivity detector and a Metrosep A Supp 7 column together with a background electrolyte containing 5% acetonitrile and 3.6 mM sodium carbonate. DO was measured using an oxygen electrode (INESA JPST-605F, China) calibrated with deoxygenated water and air-saturated water at room temperature. BET surface area was observed by a porosimetry analysis (Micromeritics Tristar 3020 II, USA). To detach corrosion coatings, iron particles were conducted in an ultrasonic cleaner (Kun Shan KQ-500DB, China) at 200 W power lasting for 10 min (Zhuang and Huang, 2006). After filtration, both suspended precipitates and surface coatings were prepared for X-ray diffraction (XRD) (Rigaku Dmax 2500, Japan) and scanning electron

microscope (SEM) (Carl Zeiss Merlin, Germany).

2.6. Experimental result expression

The pseudo-first order model (1) was applied to describe the removal of CAA in reaction system since iron particles used was kept in excess (10 g/L) toward each CAA (25 μM).

$$C = C_0 e^{-kt} \quad (1)$$

Where C was the CAA concentration (μM) at any reaction time t (min), C_0 was the initial CAA concentration (μM), k was the pseudo-first-order rate constant (min^{-1}). The observed pseudo-first-order rate constants were determined from the slope of the linear regressions obtained by plotting $\ln(C/C_0)$ versus reaction time,

3. Results

3.1. Dissolved oxygen concentration

When the reactor headspace was periodically refreshed using above-mentioned procedures, the DO concentration was kept stable at 0, 0.75 ± 0.14, 1.52 ± 0.17, 2.59 ± 0.23, 3.47 ± 0.25, and 7.09 ± 0.83 mg/L (Fig. 1). The negligible DO concentration detected in the anoxic system could be attributed to the O_2 dissolution during determination.

3.2. CAA removal and reaction kinetics

The effect of DO concentration on the reduction of CAAs by iron was shown in Fig. 2. When the DO concentration was at 0, 0.75, 1.52, 2.59 3.47 and 7.09 mg/L, the final removal efficiency of MCAA was 1.25%, 19.6%, 27.5%, 21.3%, 19.9% and 14.4%, and that of DCAA was 26.1%, 64.2%, 68.1%, 49.4%, 43.9% and 22.4%, and that of

TCAA was 77.2%, 80.5%, 75.3%, 54.4%, 42.0% and 26.0%, respectively. It was found that gradually increasing DO concentration in the reactor, the CAA removal efficiency increased first and then decreased. The optimum DO concentration for the MCAA and DCAA reduction was 1.52 mg/L and that for the TCAA reduction was 0.75 mg/L.

As shown in Table 1, owing to the O_2 supplement, the rate constant for MCAA was dramatically enhanced at three orders of magnitude higher than that under the anoxic condition. MCAA removal was insensitive to the change in DO concentration under oxic conditions, for similar rate constants in the range 1.35-2.73 × 10^{-3} min^{-1}. The rate constants for DCAA detected at 0 and 7.09 mg/L were obviously lower than those ranged from 5.02 × 10^{-3} to 8.85 × 10^{-3} min^{-1} at residual DO concentrations. TCAA was quickly removed at DO concentrations below 2.59 mg/L. The removal of TCAA was significantly inhibited by further increasing DO concentration, for its rate constant of 2.95 × 10^{-3} min^{-1} at the highest DO concentration was nearly one fourth of 10.22 × 10^{-3} min^{-1} in the absence of O_2. The susceptibility of CAAs to iron at all DO concentrations strictly followed the order of TCAA, DCAA, and lastly MCAA, probably influenced by the number of substituent chlorine (Li et al., 2012; Zhang et al., 2004). However, the susceptibility of CAA reduction improved by O_2 followed the order of MCAA, DCAA, and lastly TCAA. The differences in observed rate constants for CAAs gradually decreased with the increase of DO concentration, especially for approximate rate constants for DCAA and TCAA at the same DO above 2.59 mg/L.

The degradation process of CAAs was composed of their mass transfer from

bulk water to particle surface, migration across the corrosion coatings and subsequent redox reaction. The overall mass transfer coefficient for MCAA, DCAA and TCAA was calculated at 0.202, 0.184 and 0.170 min^{-1}, respectively. Details of the computations were supplied in the appendix A. Since the ratio of observed rate constant to overall mass transfer coefficient was 0.07 at most, the three CAAs were not belonged to mass transfer limited species. Therefore, the migration or reduction of CAAs would become the limiting step in their degradation processes, which might vary with the DO concentration.

3.3. CAA degradation processes

TCAA degradation processes influenced by various DO concentrations were shown in Fig. 3. The removal processes of both MCAA and DCAA were also provided in the appendix B. At DO concentrations less than 2.59 mg/L, the amount of TCAA reduction was similar and ranged from 19.97 to 21.49 μM. However, there was obvious difference in its dechlorination products. TCAA was transformed into 16.92 μM DCAA, 3.66 μM MCAA and 0.46 μM AA without O_2. The accumulation of DCAA was related to its low rate constants under the anoxic condition. TCAA was dechlorinated into 5.31 μM DCAA, 13.20 μM MCAA and 3.50 μM AA at 0.75 mg/L DO, and 3.81 μM DCAA, 11.12 μM MCAA and 4.98 μM AA at 1.52 mg/L DO. Under these low oxic conditions, MCAA became the main TCAA degradation product, companying with a notable increase in the AA formation. This phenomenon might result from the enhanced rate constants for various CAAs. The reduction of TCAA and generation of corresponding products were impeded under high oxic conditions,

while MCAA was maintained as the major product. During a 2-h reaction period, the amount of AA formation gradually exceeded the DCAA concentration in the DO range 1.52-3.47 mg/L. Owing to the different rate constants for CAAs affected by O_2, the distribution law of TCAA degradation products varied at various DO concentrations.

In this study, the mass balance of total carbon (i.e. the sum of AA and all CAAs) was 92-105% in all anoxic and oxic systems. Therefore, CAAs were mainly removed by the chemical degradation within the system. The total chlorine consisted of the chloride ion measured by IC and combined chlorine calculated from CAAs. The mass balance of total chlorine was only detected in the anoxic systems, 69-95% for other oxic systems. Based on the carbon mass balance, the combined chlorine content in CAAs was stable, so the total chlorine loss resulted from a decrease in the chloride ion, probably involved in the dissolution of corrosion products (Lytle et al., 2005; Moore and Yong, 2005) or trapped within the lattice structure of oxides (Gilberg and Seeley, 1981).

The oral LD_{50} (lethal dose causing 50% mortality) in rats for TCAA, DCAA, MCAA and AA is 3320, 2820, 55 and 3310 mg/kg, respectively, which indicated that the formation of MCAA or DCAA might increase the biological toxicity of raw water. Combined to their biodegradability (Tang et al., 2013), AA was the most desirable product from the degradation of CAAs by iron. As shown in Fig. 4, the formation of AA during CAA degradation was enhanced first and then partly hindered with an increase of DO concentration, and the optimum DO concentration was 1.52 mg/L.

3.4. Iron and corrosion products

As shown in Fig. 5, the raw iron was mainly composed of zero-valent iron based on the XRD analysis. After hermetically storing in water for a period, the iron particles used had been covered with a significant amount of magnetite, presenting a dense surface with cracks from the SEM image. Under the anoxic condition, both suspended precipitates and surface coatings were identified as magnetite (Fe_3O_4), which was showed as black partly rounded crystals. The detected sheet or platy structure might result from part oxidation during determination. Under the oxic conditions, lepidocrocite (γ-FeOOH) and magnetite were simultaneously determined in suspended precipitates while magnetite was the sole mineral in surface coatings, probably for the insufficient amounts of lepidocrocite on the surface of iron particles. The weak adherence of lepidocrocite might related to its irregular plates morphology. Lepidocrocite as a visible brownish-yellowish precipitate was only observed in the presence of O_2.

The change of CAA concentration was observed in solution containing specific corrosion products. Details of preliminary experiment processes and results were supplied in the appendix C. Negligible loss of CAAs under neutral condition were observed in the presence of synthetic or mixed corrosion products with/without ferrous iron, which was accordant with other report (Chun et al., 2005). The amount of Fe^{II} detached from iron core was supposed to zero for its rapid oxidation by aqueous O_2 at pH above 7 (Morgan and Lahav, 2007). Combined with carbon recovery mentioned above, the adsorption or reduction of CAAs by suspended

corrosion products was limited in this study.

The removal of CAAs by iron with acid pretreatment was carried out to investigate the role of corrosion coatings as shown in Fig. 6. The decreasing order of iron efficiency over 2 h of reaction toward three CAAs was: iron with oxic corrosion coatings > iron with anoxic corrosion coatings > fresh iron. TCAA and DCAA could be partly removed by green rust as oxic corrosion rather than by magnetite (Chun et al., 2005, 2007), which might prove powerful reductants formed in oxic systems. At end of removal experiment, there was no substantial decrease of DCAA in the fresh iron system and almost no loss of MCAA in the absence of O_2, while considerable AA was formed in the presence of O_2. This comparison suggested that corrosion coatings on the surface of Fe^0 core were responsible for the evolution of CAA removal efficiency within various iron/water systems.

4. Discussions

Due to the mechanical abrasion in well-mixed batch systems, a thin layer of corrosion coatings was expected on the core of Fe^0 (Zhang and Huang, 2006). The corrosion product in the ferrous state (FeO) was expected to be closest to the core (Noubactep, 2008; Sarin et al., 2004b). The black green solution of iron corrosion at the high stirring speed and loss of chlorine mass balance under oxic conditions could be a sign of the presence of green rust, which was common intermediate species of chemical oxidation of ferrous to ferric iron by O_2 and ultimately transformed into stable lepidocrocite (Morgan and Lahav, 2007; Westerhoff and James, 2003). Combined with the observation of XRD and SEM, two structure of corrosion coatings

were proposed to explain the CAA removal mechanism under the anoxic and oxic conditions in Fig. 7.

As a possible limiting step, the migration of CAAs across the corrosion coatings primarily depended on film permeability and affinity between contaminants and corrosion oxides (Nesic, 2007; Noubactep, 2008; Noubactep, 2012). The dissolution constant (pKa) of CAAs was in the range of 0.51-2.87 and the point of zero charge (pHpzc) of magnetite and lepidocrocite were 6.4-6.9 and 7.3 (Pecher et al., 2002). At pH range of 7-9 in this study, both CAAs and iron corrosion product were negatively charged. Hence, the weak affinity was helpful to the migration of CAAs and their products in corrosion coatings. The porosity (or permeability) against density increased from metal towards the outer surface of oxide film, and the density of oxide decreased with increasing oxygen content in its chemical structural. Higher O_2 availability would lead a larger volumetric expansion and longer migration path (Domga et al., 2015). The calculated diffusion coefficients of 10^{-12}-10^{-16} cm^2/s were compatible with ion diffusion through a semi-porous substrate (White et al., 1994). It seemed to be very important for subsequent electrochemical or chemical reduction.

As the other possible limiting step, the reduction of CAAs was related to available reducing agents, which originated from iron corrosion affected by the electronic and ionic properties of surface oxides (Sato, 2001). The quantitative contaminant directly removed by Fe^0 core was nonrealistic due to dense corrosion coatings decreasing the accessibility of Fe^0 surface (Noubactep, 2008). However, contaminant removal through electrons was feasible since the FeO, Fe_3O_4 and/or

green rust layer were electronic conductive (O'Carroll et al., 2013; Yan et al., 2010), while few electrons could penetrate the outer lepidocrocite layer (the band gap of 2.3 eV). In addition to structural Fe^{II} in iron (oxy)hydroxides, the electronegative oxides were easy to adsorb aqueous cations and then to form indirect reducing agents that are more powerful than Fe^{0}, such as atom hydrogen or absorbed Fe^{II}, with -0.65~-0.34 V for Fe^{II} compared to -0.44 V for Fe^{0} (White and Peterson, 1996; Noubactep, 2012). Surface complex attached Fe^{II} might be helpful to the adsorption of CAA ion from the aqueous solution by the electromotive force. The formation of oxidized layers (such as γ-FeOOH) on structural or absorded Fe^{II} oxides diminished the rates of aqueous metal reduction due to the required transfer of both electrons and Fe^{II} from the underlying unoxidized mineral to the aqueous interface (White and Peterson, 1996), which leaded to no significant loss of CAAs by suspended corrosion products. Hence, only oxides with continuous replenishment of electron and Fe^{II} could rapidly reduce CAAs, as the conductive layer coated on the surface of Fe^{0} core. Certainly, it was necessary for the reduction of contaminants to penetrate the outer nonconductive layer. The diffusion or migration of CAAs within the conductive layers as reactive interfaces was not considered in this study.

The reduction of CAAs by iron was shown in the equation (2), and their removal rates were dependent on the available reductants and CAAs on the reactive surface (Noubactep et al., 2010).

$$\text{Reductants}_{\equiv} + \text{CAAs}_{\equiv} \rightarrow \text{CAA or AA} + \text{Cl}^{-} \qquad (2)$$

The reducing agents for CAAs under anoxic and oxic conditions was shown in

the following equations (3). In addition to forming solid corrosion products, soluble ferrous iron was released into bulk water by penetrating the little cracks in the oxide layer, and possibly through atom exchange with the ferrous in lattice (Cwiertny et al., 2008; Pedersen et al., 2005). This diffusion rate decreased with increasing concentration of aqueous ferrous iron, eventually slowing the rate of iron corrosion and electron release.

$$\mathrm{Fe}^{0} \rightarrow \mathrm{Fe}^{2+} + e \xrightarrow{\text{Anoxic}} \mathrm{Fe}^{\mathrm{II}}, e, \mathrm{H}_{\equiv \mathrm{FeO}, \mathrm{Fe}_3\mathrm{O}_4} \xrightarrow{\text{Oxic}} \mathrm{Fe}^{\mathrm{II}}, e, \mathrm{H}_{\equiv \mathrm{FeO}, \mathrm{Fe}_3\mathrm{O}_4, \text{Green rust}} \quad (3)$$

A relationship of CAA concentration on the conductive surface and in bulk solution was roughly functioned as the thickness (*d*) of outer lepidocrocite layer attached, as depicted in the equation (4). When the thickness was equal to 0, the value of function was 1. The function value gradually dropped to zero with the continuous growth of lepidocrocite coating.

$$\mathrm{CAAs}_{\equiv} = \mathrm{CAAs}_{\mathrm{bulk}}\, f(d_{\gamma-\mathrm{FeOOH}}) \quad (4)$$

The addition of reducing agents such as $\mathrm{Fe}^{\mathrm{II}}$ or H absorbed on various oxides(Ghauch et al., 2010; Gheju and Balcu, 2011), enhanced dramatically the removal of CAAs, for decreasing order of iron efficiency: iron with oxic corrosion coatings > iron with anoxic corrosion coatings > fresh iron. Under the anoxic condition, CAAs on the magnetite surface were the same as bulk concentrations due to the absence of lepidocrocite. Because the accumulation of aqueous ferrous iron, approximate 7.28 μM detected in this study, gave a negative feedback to corrosion of iron, the degradation of CAAs was limited by available reductants. Under the low oxic condition, the reduction of O_2 by ferrous iron was dominating, with the

formation of powerful green rust (Stratmann and Müller, 1994). The aqueous ferrous iron could barely be detected above 1.52 mg/L DO, which would lead to additional electron release. Li and Farrell (2000) reported the cell current was increased from 11 to 18 mA, while the DO concentration was rising from 0 to 9 mg/L. The adverse effect of lepidocrocite could be postponed by transforming into magnetite (Kuch, 1988; Ritter et al., 2003; Tamaura et al., 1983). These advantages were remarkable in the low oxic system, resulting in a notable increase in rate constants for CAAs. Under the high oxic condition, the high reactivity of redundant O_2 with reductants and significant growth of lepidocrocite coating became the restricting factors of CAA removal. This phenomenon was confirmed by similar degradation rate constants for DCAA and TCAA. These findings have great potential in analyzing the effect of DO concentration on iron reactivity towards the removal of other contaminants in drinking water, domestic or industrial wastewater.

Conclusions

The removal of CAAs by iron increased first and then decreased with increasing the DO concentration from 0 to 7.09 mg/L. The susceptibility of CAA reduction improved by O_2 followed the order of MCAA, DCAA, and lastly TCAA. As a desirable CAA degradation product, AA was optimally transformed at 1.52 mg/L DO. The variation of available reducing agents and corrosion coatings was responsible for CAA removals at various DO concentrations. Various CAA removal mechanisms facilitate the preliminary prediction on the effect of DO concentration on iron efficiency towards the treatment of contaminants in surface water and wastewater.

Acknowledgement

The authors wish to acknowledge the financial support from National Natural Science Foundation of China (No. 51290284, 51278269). The authors are also very thankful to the anonymous reviewers who really helped in improving the quality of this manuscript.

Appendices: Supplementary data

Supplementary data associated with this article can be found in the online version.

References

Coelho, D.S.F., Ardisson, J.D., Moura, F.C., Lago, R.M., Murad, E., Fabris, J.D., 2008. Potential application of highly reactive Fe(0)/Fe3O4 composites for the reduction of Cr(VI) environmental contaminants. Chemosphere 71 (1), 90-96.

Cho, D.W., Chon, C.M., Jeon, B.H., Kim, Y., Khan, M.A., Song, H., 2010. The role of clay minerals in the reduction of nitrate in groundwater by zero-valent iron. Chemosphere 81 (5), 611-616.

Cwiertny, D.M., Handler, R.M., Schaefer, M.V., Grassian, V.H., Scherer, M.M., 2008. Interpreting nanoscale size-effects in aggregated Fe-oxide suspensions: Reaction of Fe(II) with Goethite. Geochimica et Cosmochimica Acta 72 (5), 1365-1380.

Chitrakar, R., Tezuka, S., Sonoda, A., Sakane, K., Ooi, K., Hirotsu, T., 2006. Phosphate adsorption on synthetic goethite and akaganeite. Journal of Colloid and Interface Science 298(2), 602-608.

Chun, C.L., Hozalski, R.M., Arnold, W.A., 2005. Degradation of drinking water

disinfection byproducts by synthetic goethite and magnetite. Environmental Science and Technology 39(21), 8525-8532.

Chun, C.L., Hozalski, R.M., Arnold, W.A.,2007. Degradation of disinfection byproducts by carbonate green rust. Environmental Science and Technology 41(5), 1615-1621.

Cundy, A.B., Hopkinson, L., Whitby, R.L.,2008. Use of iron-based technologies in contaminated land and groundwater remediation: a review. Science of Total Environment 400(1-3), 42-51.

Domga, R., Togue-Kamga, F., Noubactep, C., Tchatchueng, J.B., 2015. Discussing porosity loss of Fe^0 packed water filters at ground level. Chemical Engineering Journal 263, 127-134.

Fu, F., Dionysiou, D.D., Liu, H., 2014. The use of zero-valent iron for groundwater remediation and wastewater treatment: a review. Journal of Hazardous Materials 267, 194-205.

Ghauch, A., Abou Assi, H., Bdeir, S., 2010. Aqueous removal of diclofenac by plated elemental iron: bimetallic systems. Journal of Hazardous Materials 182(1-3), 64-74.

Ghauch, A., Assi, H.A., Baydoun, H., Tuqan, A.M., Bejjani, A., 2011. Fe0-based trimetallic systems for the removal of aqueous diclofenac: Mechanism and kinetics. Chemical Engineering Journal 172(2-3), 1033-1044.

Gheju M., Balcu I., 2011. Removal of chromium from Cr(VI) polluted wastewaters by reduction with scrap iron and subsequent precipitation of resulted cations.

Journal of Hazardous Materials 196, 131-138.

Gilberg, M.R., Seeley, N.J., 1981. The identity of compounds containing chloride ions in marine iron corrosion products: a critical review. Studies in conservation 26(2), 50-56.

Gillham, R.W., O'Hannesin, S.F., 1994. Enhanced degradation of halogenated alophatics by zero-valent iron. Groundwater 32(6), 958-967.

Gunawardana, B., Singhal, N., Swedlund, P., 2011. Degradation of chlorinated phenols by zero valent iron and bimetals of iron: a review. Environmental Engineering Research 16(4), 187-203.

Helland, B.R., Alvarez, P.J., Schnoor, J.L., 1995. Reductive dechlorination of carbon tetrachloride with elemental iron. Journal of Hazardous Materials 41 (2), 205-216.

Henderson, A.D., Demond, A.H., 2007. Long-term performance of zero-valent iron permeable reactive barriers: a critical review. Environmental Engineering Science 24(4), 401-423.

Huang, Y.H., Zhang, T.C., 2005. Effects of dissolved oxygen on formation of corrosion products and concomitant oxygen and nitrate reduction in zero-valent iron systems with or without aqueous Fe^{2+}. Water Research 39 (9), 1751-1760.

Huang, Y.H., Zhang, T.C., 2006. Nitrite reduction and formation of corrosion coatings in zerovalent iron systems. Chemosphere 64 (6), 937-943.

Jung, H., Kwon, K., Lee, E., Kim, D., Kim, G., 2011. Effect of dissolved oxygen on corrosion properties of reinforcing steel. Corrosion Engineering, Science and

Technology 46(2), 195-198.

Kim, E.J., Murugesan, K., Kim, J.H., Tratnyek, P.G., Chang, Y.S., 2013. Remediation of Trichloroethylene by FeS-Coated Iron Nanoparticles in Simulated and Real Groundwater: Effects of Water Chemistry. Industrial and Engineering Chemistry Research 52 (27), 9343-9350.

Kuch, A., 1988. Investigations of the reduction and re-oxidation kinetics of iron (III) oxide scales formed in waters. Corrosion Science 30 (3), 221-231.

Lee, J.Y., Hozalski, R.M., Arnold, W.A., 2007. Effects of dissolved oxygen and iron aging on the reduction of trichloronitromethane, trichloracetonitrile, and trichloropropanone. Chemosphere 66 (11), 2127-2135.

Li, A., Zhao, X., Hou, Y., Liu, H., Wu, L., Qu, J., 2012. The electrocatalytic dechlorination of chloroacetic acids at electrodeposited Pd/Fe-modified carbon paper electrode. Applied Catalysis B: Environmental 111-112, 628-635.

Li, L., Fan, M., Brown, R.C., Van Leeuwen, J., Wang, J., Wang, W., Song, Y., Zhang, P., 2006. Synthesis, Properties, and environmental applications of nanoscale iron-based materials: a review. Environmental Science and Technology 36(5), 405-431.

Li, T., Farrell, J., 2000. Reductive dechlorination of trichloroethene and carbon tetrachloride using iron and palladized-iron cathodes. Environmental Science and Technology 34 (1), 173-179.

Lytle, D.A., Sarin, P., Snoeyink, V.L., 2005. The effect of chloride and orthophosphate on the release of iron from a cast iron pipe section. Journal of Water Supply:

Research and technology 54 (5), 267-281.

Mak, M.S., Lo, I.M., Liu, T., 2011. Synergistic effect of coupling zero-valent iron with iron oxide-coated sand in columns for chromate and arsenate removal from groundwater: Influences of humic acid and the reactive media configuration. Water Research 45 (19), 6575-6584.

Matheson, L.J., Tratnyek, P.G., 1994. Reductive dehalogenation of chlorinated methanes by iron metal. Environmental Science and Technology 28(12), 2045-2053.

Moore, A.M., Young, T.M., 2005. Chloride interactions with iron surfaces: implications for perchlorate and nitrate remediation using permeable reactive barriers. Journal of Environmental Engineering 131 (6), 924-933.

Morgan, B., Lahav, O., 2007. The effect of pH on the kinetics of spontaneous Fe (II) oxidation by O_2 in aqueous solution – basic principles and a simple heuristic description. Chemosphere 68(11), 2080-2084.

Nesic, S., 2007. Key issues related to modelling of internal corrosion of oil and gas pipelines – a review. Corrosion Science 49(12), 4308-4338.

Noubactep, C., 2008. A critical review on the process of contaminant removal in Fe^0–H_2O systems. Environmental Technology 29 (8), 909-920.

Noubactep, C., 2010. The suitability of metallic iron for environmental remediation. Environmental Progress & Sustainable Energy 29(3), 286-291.

Noubactep, C., 2011. Aqueous contaminant removal by metallic iron: Is the paradigm shifting? Water SA 37(3), 419-426.

Noubactep, C., 2012. Investigating the processes of contaminant removal in Fe^0/H_2O systems. Korean Journal of Chemical Engineering 29(8), 1050-1056.

Noubactep, C., 2014. Flaws in the design of Fe(0)-based filtration systems? Chemosphere 117, 104-107.

Noubactep, C., Care, S., Crane, R., 2012. Nanoscale Metallic Iron for Environmental Remediation: Prospects and Limitations. Water, Air, and Soil Pollution 223(3), 1363-1382.

Noubactep, C., Schöner, A., Sauter, M., 2010. Significance of oxide-film in discussing the mechanism of contaminant removal by elemental iron materials. Photo-Electrochemistry and Photo-Biology for the Sustainablity. Bentham Science Publishers, 34-55.

O'Carroll, D., Sleep, B., Krol, M., Boparai, H., Kocur, C., 2013. Nanoscale zero valent iron and bimetallic particles for contaminated site remediation. Advances in Water Resources 51, 104-122.

Pecher, K., Haderlein, S.B., Schwarzenbach, R.P., 2002. Reduction of polyhalogenated methanes by surface-bound Fe(II) in aqueous suspensions of iron oxides. Environmental Science and Technology 36(8), 1734-1741.

Pedersen, H.D., Postma, D., Jakobsen, R.. Larsen, O., 2005. Fast transformation of iron oxyhydroxides by the catalytic action of aqueous Fe(II). Geochimica et Cosmochimica Acta 69 (16), 3967-3977.

Rahman, M.S., Gagnon, G.A., 2014. Bench-scale evaluation of drinking water treatment parameters on iron particles and water quality. Water Research 48,

137-147.

Ritter, K., Odziemkowski, M., Simpgraga, R., Gillham, R., Irish, D., 2003. An in situ study of the effect of nitrate on the reduction of trichloroethylene by granular iron. Journal of Contaminant Hydrology 65 (1), 121-136.

Sarin, P., Snoeyink, V.L., Bebee, J., Jim, K.K., Beckett, M.A., Kriven, W.M., Clement, J.A., 2004a. Iron release from corroded iron pipes in drinking water distribution systems: effect of dissolved oxygen. Water Research 38 (5), 1259-1269.

Sarin, P., Snoeyink, V.L., Lytle, D.A., Kriven, W.M., 2004b. Iron corrosion scales: model for scale growth, iron release, and colored water formation. Journal of Environment Engineering 130 (4), 364-373.

Sato, N., 2001. Surface oxides affecting metallic corrosion. Corrosion Reviews 19(3-4), 253-272.

Scherer, M.M., Balko, B.A., Tratnyek, P.G., 1998. The role of oxides in reduction reactions at the metal-water interface, pp. 301-322, ACS Publications.

Schlautman, M.A., Han, I., 2001. Effects of pH and dissolved oxygen on the reduction of hexavalent chromium by dissolved ferrous iron in poorly buffered aqueous systems. Water Research 35(6), 1534-1546.

Scott, T.B., Popescu, I.C., Crane, R.A., Noubactep, C., 2011. Nano-scale metallic iron for the treatment of solutions containing multiple inorganic contaminants. Journal of Hazardous Materials 186(1), 280-287.

Song, H., Jeon, B.H., Chon, C.M., Kim, Y., Nam, I.H., Schwartz, F.W., Cho, D.W., 2013. The effect of granular ferric hydroxide amendment on the reduction of

nitrate in groundwater by zero-valent iron. Chemosphere 93 (11), 2767-2773.

Stratmann, M., Müller, J., 1994. The mechanism of the oxygen reduction on rust-covered metal substrates. Corrosion Science 36 (2), 327-359.

Tamaura, Y., Ito, K., Katsura, T., 1983. Transformation of γ-FeOOH to Fe_3O_4 by adsorption of iron(II) ion on γ-FeOOH. Journal of the Chemical Society, Dalton Transactions 1983, 189-194

Tang, S., Wang, X.M., Yang, H.W., Xie, Y.F., 2013. Haloacetic acid removal by sequential zero-valent iron reduction and biologically active carbon degradation. Chemosphere 90 (4), 1563-1567.

Uludag-Demirer, S., Bowers, A.R., 2003. Effects of surface oxidation and oxygen on the removal of trichloroethylene from the gas phase using elemental iron. Water, Air, and Soil Pollution 142 (1-4), 229-242.

Wang, H.B., Hu, C., Hu, X.X., Yang, M., Qu, J.H., 2012. Effects of disinfectant and biofilm on the corrosion of cast iron pipes in a reclaimed water distribution system. Water Research 46 (4), 1070-1078.

Wang, K.S., Lin, C.L., Wei, M.C., Liang, H.H., Li, H.C., Chang, C.H., Fang, Y.T., Chang, S.H., 2010. Effects of dissolved oxygen on dye removal by zero-valent iron. Journal of Hazardous Materials 182 (1-3), 886-895.

Westerhoff, P., James, J., 2003. Nitrate removal in zero-valent iron packed columns. Water Research 37 (8), 1818-1830.

White, A.F., Peterson, M.L., 1996. Reduction of aqueous transition metal species on the surfaces of Fe(II)-containing oxides. Geochimica et Cosmochimica Acta

60(20), 3799-3814.

White, A.F., Peterson, M.L., Hochella Jr, M.F., 1994. Electrochemistry and dissolution kinetics of magnetite and ilmenite. Geochimica et Cosmochimica Acta 58(8), 1859-1875.

Xie, L., Shang, C., 2007. The effects of operational parameters and common anions on the reactivity of zero-valent iron in bromate reduction. Chemosphere 66 (9), 1652-1659.

Yan, W., Herzing, A.A., Kiely, C.J., Zhang, W.X., 2010. Nanoscale zero-valent iron (nZVI): Aspects of the core-shell structure and reactions with inorganic species in water. Journal of Contaminant Hydrology 118(3–4), 96-104.

Yoon, I.H., Bang, S., Chang, J.S., Gyu Kim, M., Kim, K.W., 2011. Effects of pH and dissolved oxygen on Cr(VI) removal in Fe(0)/H_2O systems. Journal of Hazardous Materials 186 (1), 855-862.

Zhang, L., Arnold, W.A., Hozalski, R.M., 2004. Kinetics of haloacetic acid reactions with Fe(0). Environmental Science and Technology 38 (24), 6881-6889.

Zhang, T.C., Huang, Y.H., 2006. Profiling iron corrosion coating on iron grains in a zerovalent iron system under the influence of dissolved oxygen. Water Research 40 (12), 2311-2320

Table 1. The observed rate constants for CAAs at various DO concentrations.

DO (mg/L)	Rate constants ($\times 10^{-3}$ min^{-1}) [a]		
	MCAA	DCAA	TCAA
0	0.003 ± 0.04	1.95 ± 0.17	10.22 ± 0.75
0.75	1.82 ± 0.05	7.35 ± 0.46	12.11 ± 0.56
1.52	2.73 ± 0.04	8.85 ± 0.28	11.13 ± 0.24
2.59	2.19 ± 0.10	5.91 ± 0.11	7.19 ± 0.22
3.47	2.07 ± 0.08	5.02 ± 0.09	4.91 ± 0.11
7.09	1.35 ± 0.05	2.53 ± 0.15	2.95 ± 0.19

[a]: Errors represent 95% confidence limits.

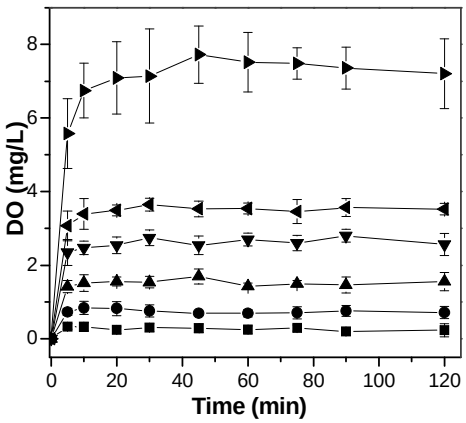

Fig. 1. Various DO concentrations at average values of 0 (■), 0.75 (●), 1.52 (▲), 2.59 (▼), 3.47 (◄) and 7.09 (►) mg/L.

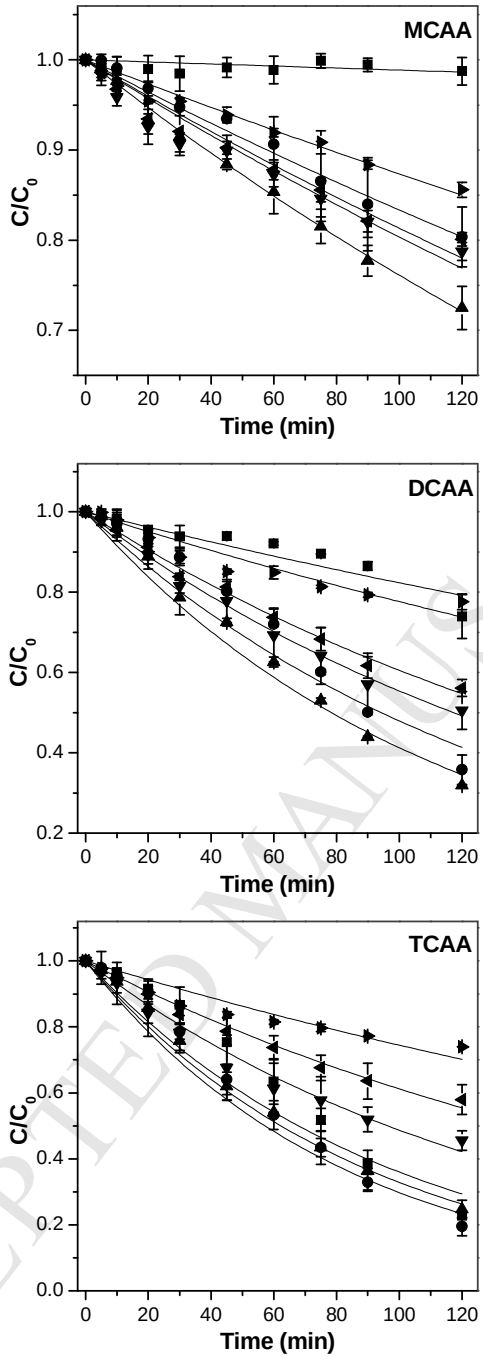

Fig. 2. Removal of CAAs by iron at various DO concentrations including 0 (■), 0.75 (●), 1.52 (▲), 2.59 (▼), 3.47 (◄) and 7.09 (►) mg/L. The solid lines were fits using the pseudo-first-order model.

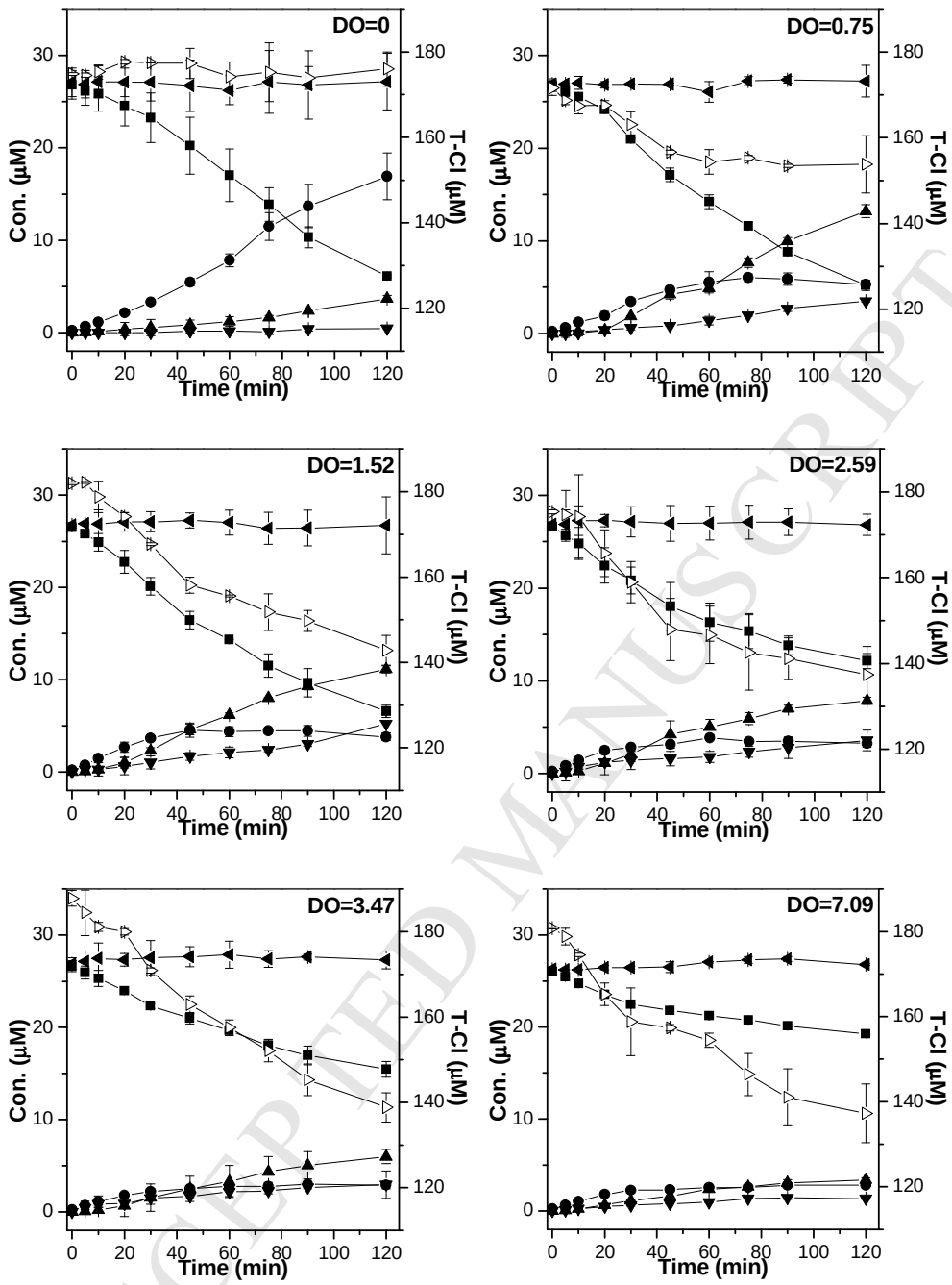

Fig. 3. Degradation of TCAA (■) by iron at various DO concentrations. Major products: DCAA (●), MCAA (▲) and AA (▼). Mass balance analyses: total carbon (◀) and total chlorine (▶).

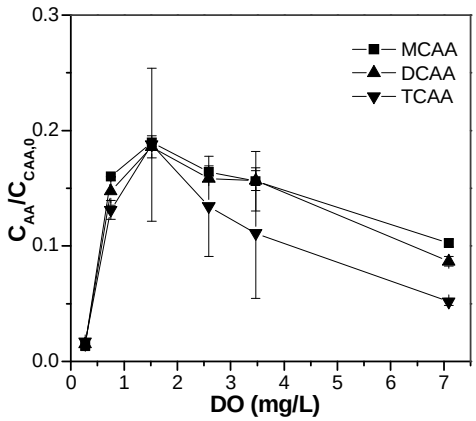

Fig. 4. Formation of AA during CAA degradation at various DO concentrations.

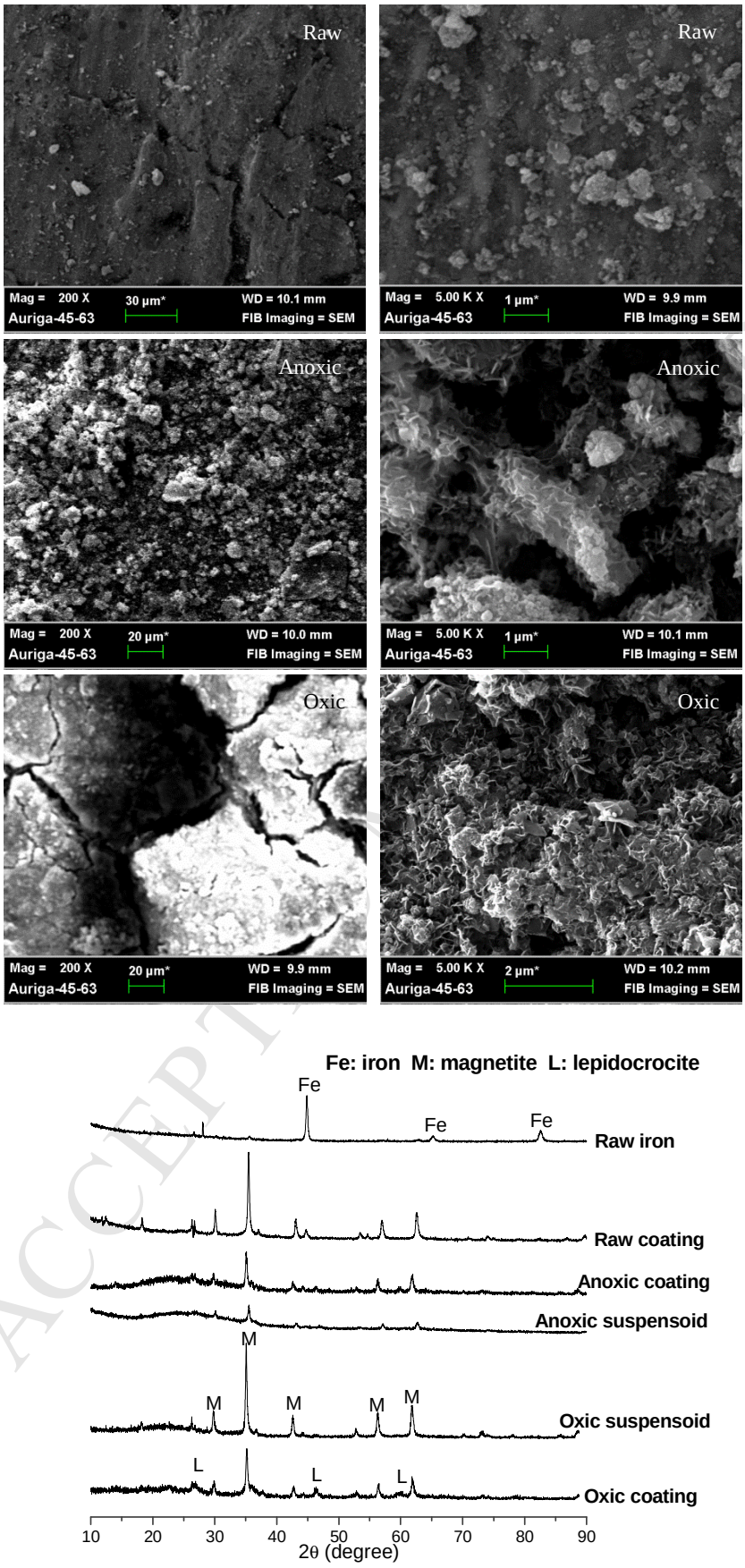

Fig. 5. SEM and XRD images of iron and corrosion products

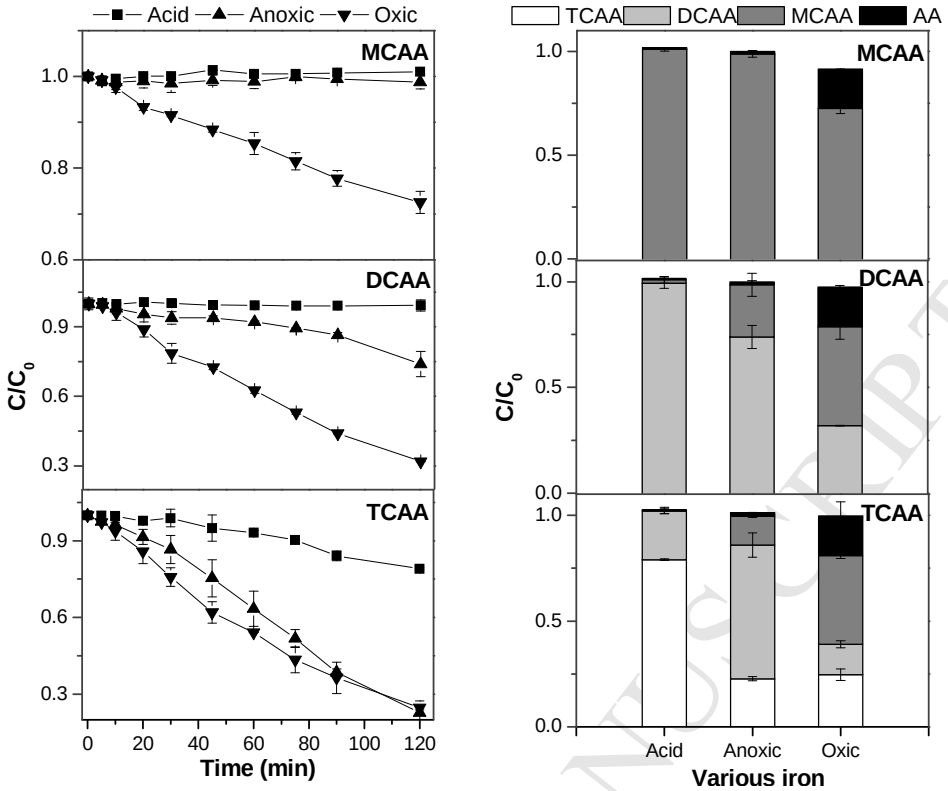

Fig. 6. Removal (Left) and degradation products at 120 min (Right) of CAAs by iron with various corrosion coatings. Acid showed iron used was without any corrosion coatings. Anoxic and oxic represented the removal of CAAs at 0 and 1.52 mg/L DO.

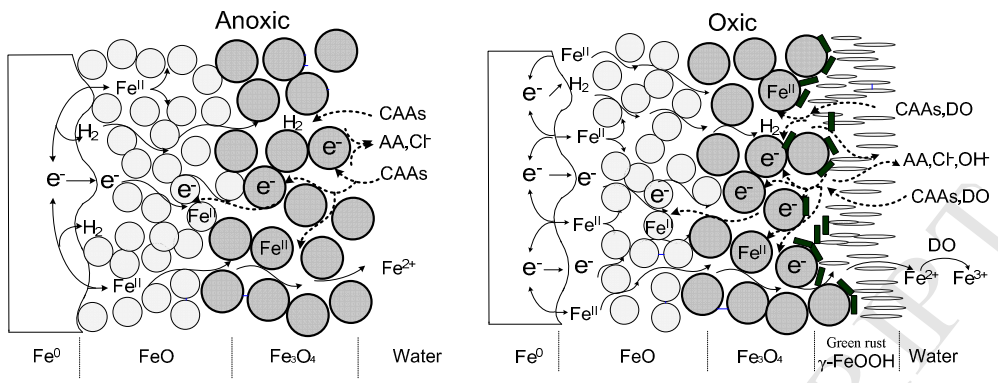

Fig. 7. Schematic representation of the removal of CAAs by iron under different conditions.

- ✓ The removal of CAAs by iron increased first and then decreased with increasing DO concentration from 0 to 7.09 mg/L.
- ✓ The maximum AA formation during three CAA degradations was obtained at 1.52 mg/L DO.
- ✓ Two structure of corrosion coatings on iron core were proposed to explain the CAA removal mechanism under anoxic and oxic conditions.

Supplementary data for

Effect of dissolved oxygen concentration on iron efficiency: Removal of three chloroacetic acids

Shun Tang[1], Xiao-mao Wang[1], Yu-qin Mao[1], Yu Zhao[1], Hong-wei Yang[1,*], Yuefeng F. Xie[1,2]

[1]State Key Joint Laboratory of Environmental Simulation and Pollution Control, School of Environment, Tsinghua University, Beijing 100084, P.R. China

[2]Environmental Programs, The Pennsylvania State University, 777 West Harrisburg Pike, Middletown, PA17057, USA

Appendix A: Computation of overall mass transfer coefficient

The ratio of observed rate constant to overall mass transfer coefficient should be calculated before determining the appropriate kinetic scenario in the mixed reactors. If the ratio is below to 0.1, the system is considered reaction limited. If the ratio is approximately equal to 1, the system is mass transfer limited. The partially reaction limited is appropriate for the residual ratios.

The overall mass transfer coefficient of solute is the sum of corrected mass transfer rate, k_m* (m/s), multiplied by the geometric surface area of the metal per volume of solution, a (m^2/m^3), as described in following equation (A-1) (Crittenden et al., 2012; Harriott, 2003). A correction factor of 1.5 adjusting minimum mass transfer coefficient k_m (m/s) is suggested to for a system mixed by recirculating liquid (Harriott, 1962; Zhang et al., 2004).

$$k_{overall} = k_m^{*} a = 1.5 \times k_m a \qquad \text{(A-1)}$$

The minimum mass transfer coefficient is calculated using the empirical correlation as follows (A-2).

$$Sh = \frac{k_m d_p}{D_w} = 2 + 0.6\,\mathrm{Re}^{1/2}\, Sc^{1/3} \qquad \text{(A-2)}$$

Where *Sh*, *Re* and *Sc* are the Sherwood number, the Reynolds number and the Schmidt number, respectively. The latter two parameters are expressed in equation (A-3) and (A-4).

$$\mathrm{Re} = \frac{d_p u_t \rho}{\mu} \qquad \text{(A-3)}$$

$$Sc = \frac{\mu}{\rho D_w} \qquad \text{(A-4)}$$

Where d_p is the particle diameter of iron (m), ρ and μ is the density (kg/m^3) and viscosity (Pa·s) of the fluid, D_w is the diffusion coefficient of specific solute in water (m^2/s), u_t is the terminal settling velocity of particles (m/s). The value of u_t can be calculated via the equation (A-5) (Zhang et al., 2004; Wang and Zhu, 2010).

$$u_t = [\frac{2g}{27}(\frac{\rho_p}{\rho} - 1)]^{\frac{5}{7}} d_p^{\frac{8}{7}} (\frac{\mu}{\rho})^{-\frac{3}{7}} \quad \text{(A-5)}$$

In which g is gravitational acceleration 9.8 m/s^2, and ρ_p is the density of solid particles (kg/m^3).

For our system, a d_p of 0.0005 m was estimated and a ρ_p of 7.86×10^3 kg/m^3 for zero-valent iron was adopted. Therefore, the external surface area assuming spherical particles was 1.527 × 10^{-3} m^2/g and corresponding a was supposed to 15.27 m^2/m^3 due to the iron loading of 10 g/L.

The ρ and μ were 0.9970×10^3 kg/m^3 and 0.8937×10^{-3} Pa·s for water at 25 °C. The diffusion coefficient of MCAA, DCAA and TCAA in the similar system has been reported at 1.215×10^{-5}, 1.057×10^{-5} and 0.9445×10^{-5} cm^2/s, respectively (Wang and Zhu, 2010). The u_t and relevant Re were computed at 0.208 m/s and 116, respectively. The residual parameters of various CAAs for the mass transfer were listed in Table A-1.

Table A-1 Mass transfer parameters for the degradation of CAAs by iron

Compounds	Sc	Sh	k_m (×10^{-4} m/s)	$k_{overall}$ (min^{-1})
MCAA	737.74	60.41	1.47	0.202
DCAA	848.01	63.19	1.34	0.184

TCAA	949.02	65.53	1.24	0.170

References

Crittenden, J.C., Trussell, R.R., David, W., Hand, D.W., Howe, K.J., Tchobanoglous, G., 2005. MWH's water treatment: Principles and design. Wiley, New Jersey.

Harriott, P., 1962. Mass transfer to particles: Part 1. Suspended in agitated tanks. AIChE J. 8, 93-102.

Harriott, P., 2003. Chemical reactor design. Marcel Dekker, New York.

Wang, W., Zhu, L., 2010. Effect of zinc on the transformation of haloacetic acids (HAAs) in drinking water. Journal of Hazardous Materials 174 (1), 40-46.

Zhang, L., Arnold, W.A., Hozalski, R.M., 2004. Kinetics of haloacetic acid reactions with Fe(0). Environmental Science and Technology 38 (24), 6881-6889.

Appendix B: Reduction of MCAA and DCAA

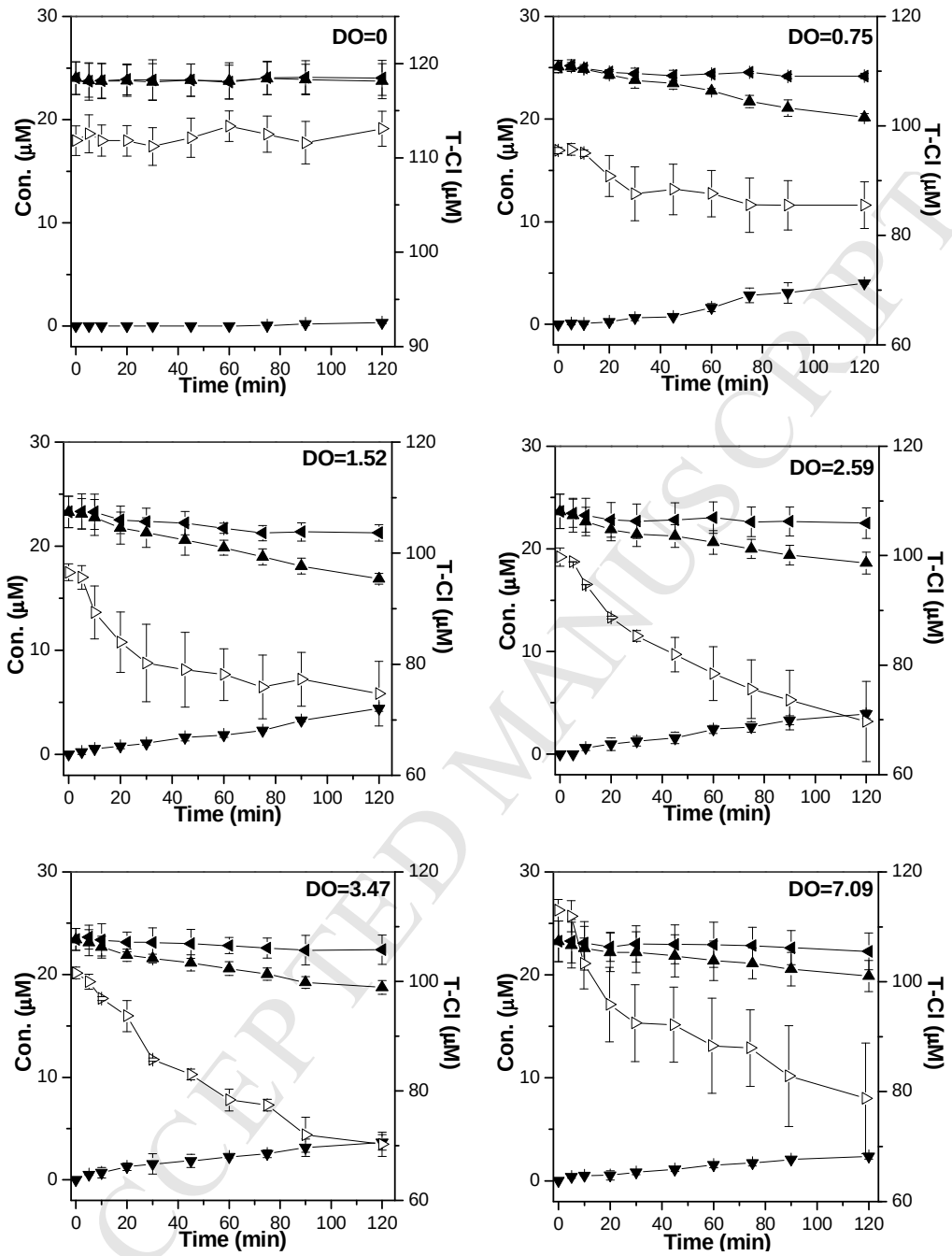

Fig. B. 1. Degradation of MCAA (▲) by iron at various DO concentrations. Major product: AA (▼). Mass balance analyses: total carbon (◀) and total chlorine (▶).

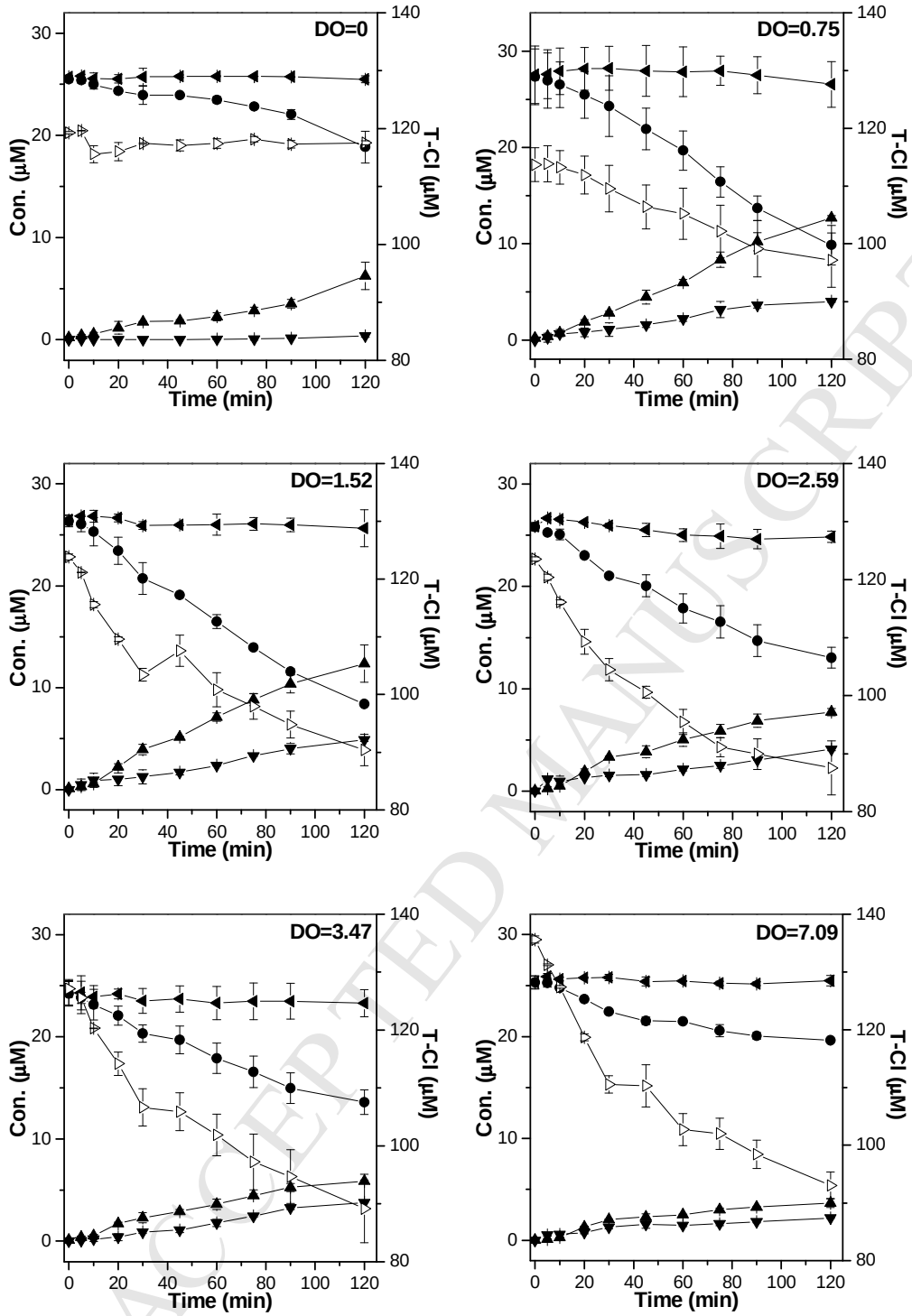

Fig. B. 2. Degradation of DCAA (●) by iron at various DO concentrations. Major products: MCAA (▲) and AA (▼). Mass balance analyses: total carbon (◀) and total chlorine (▶).

Appendix C: **The role of suspended corrosion products: preliminary test**

C.1. The removal of CAAs on synthetic iron mineral with or without ferrous iron.

The initial solution containing approximately 25 μM CAA was prepared using ultrapure water. After adjusting pH to 3.0 or 7.0, CAA solution (55 mL without N_2 purge) and corrosion products (1g/L magnetite or akaganeite and 60 mg/L ferrous ion.) were transferred into a 65-mL brown bottle under atmosphere. The bottle was sealed a screw thread cap with PTFE-faced silicone septa, and loaded onto a rotator at 40 rpm for 24 h. In this preliminary study, magnetite or akaganeite was regarded the main anoxic or oxic oxide. It should be noted a significant decrease of CAAs occurred under acid condition, while almost no loss (0.97-.99) at pH of 7.

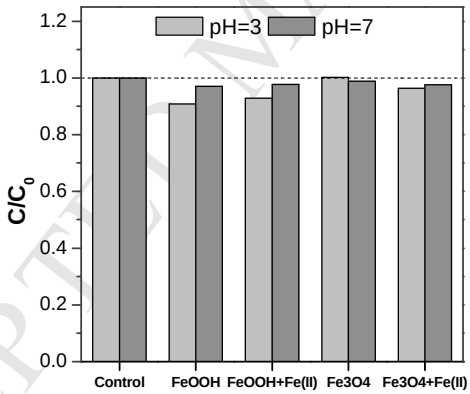

Fig. C. 1. The adsorption of CAA on iron minerals for 24 h under different pH, including 1g/L iron mineral (Magnetite or Akaganeite) and/or 60 mg/L ferrous ion.

C.2. The removal of CAAs on mixed oxic corrosion products.

A dark-green solution (55 mL, supposed to be green rust, at pH 7), formed from iron/water system stirring at 500 rpm for 2 h under atmosphere, were transferred into a 65-mL brown bottle, and then solid CAA (approximate 25 μM) was added. The bottle was sealed a screw thread cap with PTFE-faced silicone septa, and loaded onto a rotator at 40 rpm for 2 h. This preliminary study aimed to simulate the actual removal by detached oxic oxides, liking green rust and lepidocrocite. It should be noted there was no reduction of CAAs for 2 h.

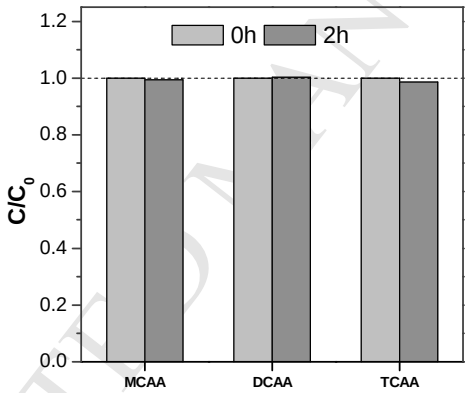

Fig. C. 2. The adsorption of MCAA, DCAA or MCAA on suspended corrosion products formed in stirring reactor with 500 rpm at approximate 4 mg/L DO.